



Report 352

June 2021

Toward Resilient Energy Infrastructure: Understanding the Effects of Changes in the Climate Mean and Extreme Events in the Northeastern United States

Muge Komurcu and Sergey Paltsev

MIT Joint Program on the Science and Policy of Global Change combines cutting-edge scientific research with independent policy analysis to provide a solid foundation for the public and private decisions needed to mitigate and adapt to unavoidable global environmental changes. Being data-driven, the Joint Program uses extensive Earth system and economic data and models to produce quantitative analysis and predictions of the risks of climate change and the challenges of limiting human influence on the environment—essential knowledge for the international dialogue toward a global response to climate change.

To this end, the Joint Program brings together an interdisciplinary group from two established MIT research centers: the Center for Global Change Science (CGCS) and the Center for Energy and Environmental Policy Research (CEEPR). These two centers—along with collaborators from the Marine Biology Laboratory (MBL) at

Woods Hole and short- and long-term visitors—provide the united vision needed to solve global challenges.

At the heart of much of the program's work lies MIT's Integrated Global System Model. Through this integrated model, the program seeks to discover new interactions among natural and human climate system components; objectively assess uncertainty in economic and climate projections; critically and quantitatively analyze environmental management and policy proposals; understand complex connections among the many forces that will shape our future; and improve methods to model, monitor and verify greenhouse gas emissions and climatic impacts.

This report is intended to communicate research results and improve public understanding of global environment and energy challenges, thereby contributing to informed debate about climate change and the economic and social implications of policy alternatives.

*—Ronald G. Prinn,
Joint Program Director*

Toward Resilient Energy Infrastructure: Understanding the Effects of Changes in the Climate Mean and Extreme Events in the Northeastern United States

Muge Komurcu¹ and Sergey Paltsev¹

Abstract: Infrastructure systems are vulnerable to weather risks. With climate change, extreme events are expected to increase. To evaluate these changes in the Northeastern United States, state-of-the-art high-resolution, convection-permitting regional climate modeling simulations are carried out to downscale projections of the Community Earth System Model (CESM) to 3 km horizontal resolution under a high impact emissions scenario for a near future time period (2025-2041). Changes in mean climate and extreme events are assessed relative to the present-day climate (2006-2020) for three key weather elements affecting electricity grid infrastructure and operations: temperatures, wind speeds and ice accumulation on infrastructure surfaces. An assessment of exceedance threshold calculations based on the safety thresholds set by National Electric Safety Code (NESC) and International Organization for Standardization (ISO) is also provided.

SUMMARY	2
1. INTRODUCTION	3
2. METHODOLOGY	3
2.1 DOWNSCALING THE EARTH SYSTEM MODEL PROJECTIONS	4
2.2 METHODS FOR ESTIMATING ICE ACCUMULATION ON INFRASTRUCTURE AND CRITICAL SURFACES	4
2.2.1 Estimation of Freezing Rain Icing	4
2.2.2 Estimation of Wet Snow Icing	5
2.2.3 Test Case Simulation of an Icing Event	5
3. CLIMATE PROJECTIONS FOR 2025-2041 AND CHANGES IN CLIMATE	6
3.1 TEMPERATURES	6
3.2 CONDITIONS FOR ICE ACCUMULATION ON SURFACES	8
3.3 WIND SPEEDS AND DIRECTION	9
4. AGGREGATE AVERAGE CHANGES IN TEMPERATURE, ICING, AND WINDS	12
5. POTENTIAL IMPACTS OF PROJECTED CHANGES ON ELECTRIC GRID INFRASTRUCTURE AND DESIGN THRESHOLDS	12
6. CONCLUDING REMARKS AND SUGGESTIONS FOR FUTURE ANALYSIS	14
7. REFERENCES	15
APPENDIX A.	16

¹ MIT Joint Program on the Science and Policy of Global Change, Massachusetts Institute of Technology.
Contact: muge@mit.edu (M. Komurcu), paltsev@mit.edu (S. Paltsev)

Summary

When on February 14, 2021, emergency was declared in Texas after a major winter storm event, which led to power failures and excessive utility bills across the state due to the sudden increase in demand, it became evident that energy infrastructure is unprepared for the changing climate conditions. With climate change, extreme heat and storm events are expected to increase. Therefore, to ensure continued safety and well-being of the communities, infrastructure design codes established based on historical climate extremes need to be revised and new policy must be established to uphold safe design and operation of critical infrastructure. Furthermore, in a changing climate, country's old and aging infrastructure must be updated to withstand future extreme events and strategic management of new and planned infrastructure must include close collaborations between commercial entities, governments, city officials owning/operating such infrastructure with atmospheric and climate scientists.

In this study, high-resolution climate projections are created and analyzed to assess physical climate risks on electricity grid infrastructure in the Northeastern United States (NE US). State of the art high-resolution, convection-permitting regional climate modeling simulations are carried out to downscale projections of the Community Earth System Model (CESM) over the NE US under a high impact emissions scenario. High-resolution (at 3km by 3km geographic scale) climate projections are generated for a near future time period (2025-2041). The resulting climate projections comprise numerous climate variables at hourly temporal resolution and are therefore suitable for use in diverse applications and assessments. Among many other climate variables, these projections include temperatures, wind speeds, wind direction, precipitation (rain and snowfall), atmospheric pressure and relative humidity. Our analysis of long term, climatic changes focus on three key weather elements affecting electricity grid infrastructure and operations: temperatures, wind speeds and icing. An offline model is deployed to estimate projected changes in icing risk (ice accumulation) on electricity grid infrastructure. The resulting projections include direct model output of 100 Terabytes and an additional 500 Gigabytes of Icing data

generated through the offline icing model. We calculate the changes relative to the present-day climate (2006-2020). Data for the present-day climate were previously generated in the same manner as our projections for a prior project and are publicly available (Komurcu *et al.*, 2018).

Physical climate risks on energy infrastructure need to be assessed at specific locations, nevertheless, we also report aggregate average changes in temperatures, icing and winds over the entire domain to provide an indication of the bulk potential changes in these climate risks in time. Based on our analysis of our projections, we find that mean temperature in NE US is 1.2°F higher in the near future (2025-2041) period relative to the present day (2006-2020) climate. We find larger changes in extreme statistics such as extreme winter temperatures in our projections. For icing indicators, we detect an increase in annual freezing rain days (~0.3 days for the domain average) and a decrease in annual wet snow days (~13.2 days change for the domain average) over the Northeastern United States. For winds, changes in the mean and extreme wind speeds are relatively small between the near future (2025-2041) and present day (2006-2020) in our projections.

We also provide several exceedance calculations over the Northeastern U.S. based on the safety thresholds set by National Electric Safety Code (NESC) and International Organization for Standardization (ISO). A more comprehensive analysis using our projections should be performed on the specific location of the asset in collaboration with the asset managers to make informed management decisions. Understanding future climate conditions is imperative for electric utilities.

Our high-resolution climate projections, while state-of-the-art, are computationally expensive to apply to downscale projections from more than one Earth system model (ESM) or under more scenarios. We call for increased support for further high-resolution climate modeling studies to include downscaling of climate projections from several ESMs which would provide a range of potential future changes in climate hence framing the uncertainty and presenting the decision makers with robust science-based information about the safety of infrastructure investments and operations.

1. Introduction

Impacts of global warming vary from region to region and are significantly different than the global scale effects (e.g. Flato *et al.*, 2013). For example, while some regions such as coastal Massachusetts experience more frequent and intense storms, precipitation or flooding events, others such as California go through more dry periods with increased heat and wildfire events (e.g. Blunden *et al.*, 2018). Changes in climate and extreme events not only threaten the lives and well-beings of the residents of these regions, but also pose a threat to the maintenance and sustainability of infrastructure such as the energy and transportation systems (e.g. Wilbanks *et al.*, 2013). More frequent and intense snowfall and flooding events create additional burdens on the city, state and utility company budgets. Adequate planning for such events allows companies to optimize funding and result in the resilient management of infrastructure.

Infrastructure systems are vulnerable to changes in the mean climate and extreme events. Increasing frequency of extreme events under climate change make it economically difficult to respond to, recover from and rebuild after such events. For grid companies, changing load patterns (from expansion of renewables and electric cars) and the impacts of climate change (changes in the mean climate characteristics and extreme events) add to the challenges to determine capital expenditures and operational changes to prevent outages. Therefore, understanding the likely magnitudes of changes in energy demand is important for decision makers, who are making strategic planning for energy supply and infrastructure development. While it is important to know the immediate effects of changes in seasonal, sub-seasonal climate and extreme weather events on energy infrastructure and energy demand, it is equally important to understand these changes in longer, decadal time scales to make better investment choices on the location, design, materials and management and financing of new and existing assets. Such knowledge is the key to increase the resiliency of the companies to physical and transitional risks.

In this study, we focus on the changes in the mean and extreme climate over the Northeastern United States (NE US) to help strategic asset planning and climate resilient infrastructure management. Weather/climate elements pose the most significant risks to infrastructure resilience. For example, increasing maximum temperatures and decreasing minimum temperatures may lead to equipment failures and outages. Similarly, if more frequent ice producing conditions or storms form or travel over the area of an asset, ice may accumulate on critical surfaces and may lead to equipment failures and outages. Extreme winds also affect infrastructure through direct damages to the infrastructure or by trees falling on to the transmission lines leading to outages. Hence understanding the likely

magnitudes for these stressors on infrastructure is important for the resiliency of existing infrastructure as well as for the planning of future infrastructure investment locations.

The report is organized in the following way. In Section 2 we describe the methodology for our analysis. Section 3 illustrates the results for climate projections for 2025-2041 and the changes in climate characteristics relative to the present-day climate (2006-2020). In Section 4 we provide aggregate mean impacts for the entire domain for temperatures, winds and icing. Section 5 offers an analysis of exceeding thresholds set by electrical safety and transmission planning guides for our domain. In Section 6 we provide concluding remarks and suggestions for future analysis.

2. Methodology

In climate science, Earth System Models (ESMs) are used to simulate past, present and future climate. ESMs include different components, such as land surface, atmosphere, ocean, cryosphere, to simulate the Earth's climate. Climate projections from all ESMs participating in the Coupled Model Intercomparison Project Phase 5 (CMIP5) reveal increasing global surface temperatures into the future (IPCC, 2013). Climate projections from ESMs, however, are too coarse for studying changes in climate at regional and local scales or to provide regional and local climate risk assessments (e.g. Komurcu *et al.*, 2018; 2020). Therefore, methodologies have been proposed to downscale climate model projections (e.g. Giorgo, 1990; Wilby, 1998). One such methodology is statistical downscaling, in which statistical relationships are established between historical, observed climate variables and ESM simulated historical climate variables. Downscaled variables are then obtained using ESM projections in such equations (Wilby, 1998). The downside of this methodology is that statistical relationships are assumed to remain fixed into the future. Another methodology is dynamical downscaling, where regional climate models are used with initial and boundary conditions from ESM projections to downscale ESM projections (e.g. Giorgo, 1990, Komurcu *et al.*, 2018; 2020). The regional climate models, similar to ESMs, have coupled land surface and atmospheric components and use established parameterizations based on theory, modeling and laboratory studies. Hence, climate variables evolve freely in time based on these parameterizations and feedbacks between processes occur, meaning that these models do not use stationary assumptions. As a result, dynamical downscaling is computationally more expensive, yet it can yield physical science based, robust results.

In this study we use dynamical downscaling to study climate change in the Northeastern United States and its potential impacts on the energy infrastructure. In fact, we go one step further and use a convection-permitting regional climate modeling approach, where we employ a horizontal resolu-

tion of 3 km in our regional climate model and eliminate the need to use a convection parameterization. *Hence, we use high-resolution, convection-permitting regional climate modeling to downscale projections of an ESM (the Community Earth System Model (CESM)) under a high impact emissions scenario (Representative Concentration Pathway (RCP) 8.5 for 17 years.* Due to the computational cost associated with convection-permitting regional climate modeling simulations, we downscale climate projections from one ESM and focus on the worst case, high emissions scenario. It is important to note that ideally much longer periods of analysis are desirable to make assessments of climate and climate change.

2.1 Downscaling the Earth System Model Projections

High-resolution climate projections are specifically generated for this study through the downscaling of the projections of an ESM under a high-impact emissions scenario using the Weather Research and Forecasting Model (WRF) (Skamarock *et al.*, 2008) to 3 km horizontal resolution over the Northeastern United States between 2025-2041. We use projections from the CESM, a model developed at the National Center of Atmospheric Research (NCAR), under RCP 8.5 as the driver of our WRF simulations. The reason we use CESM over other ESMs is that the particular CESM projections dataset we chose has been bias corrected at NCAR (Monaghan *et al.*, 2014; Bruyere *et al.*, 2015) and studied in the context of high-impact weather affecting the Eastern United States (Bruyere *et al.*, 2013; Komurcu *et al.*, 2018).

The regional climate modeling methodology is the same as in Komurcu *et al.* (2018) and we use the same three nested domains of 27, 9 and 3 km horizontal resolution as in Komurcu *et al.* (2018). The description of the WRF domain set up and parameterization choices are explained in extensive detail in Komurcu *et al.* (2018). Furthermore, assessments of model historical climate with respect to observations/retrievals based gridded products have been provided in Komurcu *et al.* (2018). Different from Komurcu *et al.* (2018), in this study new calculations were added to include *maximum hourly wind speeds at specific heights and direction of winds during maximum wind speeds during runtime.* We produce hourly output at 3 km horizontal resolution for all locations within the box outlined in red in **Figure 1**. In Appendix A, we provide a list of selected climate variables available in our projections, however, the full list of available variables in our output is extensive and includes numerous additional 2-dimensional (latitude-longitude) and 3-dimensional (latitude, longitude, height) variables in comparison to those listed in Appendix A.

2.2 Methods for Estimating Ice Accumulation on Infrastructure and Critical Surfaces

In the Earth's atmosphere, water molecule is present in three phases: water vapor, liquid water and ice. When conditions

are right, water vapor can form cloud droplets, or ice crystals which grow through condensation and collisions to form precipitation (Pruppacher and Klett, 2010). While cloud droplets form heterogeneously, with the aid of a cloud condensation nuclei, in atmospheric conditions, ice formation may take place both homogeneously and heterogeneously. Growth of atmospheric ice occurs through both collisions and coalescence and vapor deposition. The growth processes of ice involve microscale vapor and thermal diffusion as well as micro scale surface characteristics, which are challenging to represent in models and are therefore parameterized (Pruppacher and Klett, 2010).

In our regional climate model, a detailed ice microphysics scheme is used, where both number concentration and mass mixing ratio of five hydrometeors (cloud droplets, cloud ice, rain, snow and graupel) are simulated (Morrison *et al.*, 2009). The model setup used in our simulations has been shown to improve winter precipitation over high topography for the Northeastern United States when downscaling climate reanalysis (Komurcu *et al.*, 2018).

Similar to ice formation and growth in the atmosphere, ice can form and accumulate on infrastructure or critical surfaces when conditions are right posing risks for operational continuity. Icing, affecting electricity grid infrastructure, can occur through several ways (see Farzaneh *et al.*, 2008, for a detailed review) such as glaze icing, wet snow icing and dry snow icing. In this study, we focus primarily on freezing rain icing and wet snow icing as these are more dominant forms of ice accumulation in the Northeastern United States.

2.2.1 Estimation of Freezing Rain Icing

Several models have been proposed to estimate freezing rain icing (e.g. Jones, 1998, Musilek *et al.*, 2009, Sanders *et al.*,



Figure 1. Box outlined in red shows the extent of our highest resolution domain in the regional climate model. Model output at 3 km by 3 km resolution at hourly intervals between 2025-2041 were generated for this study.

2016) with varying degrees of complexity. In this study, we use Jones 1998 simple model to estimate radial ice thickness due to freezing rain icing because the model is based on theory (i.e. two fluxes impinging on a cylindrical surface), it is computationally efficient to use with our high-resolution projections, and it has been developed and tested in the Northeastern United States. While more detailed versions of this model involving heat fluxes also exist, we choose to use the simple version as our initial tests showed the simple version is yielding similar results to observed ice accumulation and better results compared to Sanders *et al.* (2016) model for the study area.

Jones 1998 model estimates ice accumulation around a cylindrical surface (wire) based on temperatures, wind speeds and water contents. The model considers fluxes of falling freezing rain and wind blown rain drops freezing and impinging on a wire. Hence, the equation for radial ice thickness is calculated hourly using the following equation:

$$R_{eq} = \frac{1}{\rho_i \pi} \sum_{j=1}^N [(P_j \rho_0)^2 + (3.6 V_j W_j)^2]^{1/2} \quad (1)$$

where P is precipitation [mm], W is water content and V is wind speed [m/s] and R_{eq} [mm] is the radial ice thickness (Jones, 1998). W is calculated as a function of precipitation (Jones, 1998).

$$W_j = 0.067 P_j^{0.846} \quad (2)$$

The equation is summed over all hours (j) where freezing rain precipitation is observed to obtain accumulated radial ice thickness during the freezing rain event in millimeters.

Jones 1998 formula assumes that both collision and coalescence efficiencies between rain drops and the cylindrical surface are 1, meaning that all raindrops hit the surface, stick to the surface and freeze (Jones, 1998). It also assumes that ice grows uniformly around the wire and the wind direction is perpendicular to the wire, hence ensuring maximum growth.

In our simulations, we calculate radial ice thickness for all grid points in our entire 3 km resolution domain (Figure 1) using Equation (1) when the two conditions are met simultaneously: 1) whenever rain occurs (we use model simulated hourly rainfall intensity [mm] from our simulations) and 2) temperatures are sub-freezing (we use near surface temperatures from our simulations). We continue accumulating ice using Equation (1) as long as both conditions are met. When conditions for freezing rain are no longer met, we reset the ice accumulation to zero.

2.2.2 Estimation of Wet Snow Icing

Similar to previous studies, we assume snowfall will accrete on surfaces as wet snow whenever two criteria are met (e.g. Sundin and Makkonnen, 1998): 1) snowfall occurs and 2) temperatures are above freezing. Hence, we start accreting ice as wet snow ice when both criteria are met and continue accreting as long as both conditions are satisfied. The assumption made here is that all snowfall accretes as wet snow. Our regional climate modeling provides snowfall in the output as liquid water equivalent [mm], we therefore assume a temperature dependent ice density formula commonly used in Land Surface Models (LSM) to convert liquid equivalent to ice thickness (Koren *et al.*, 1999). It is important to note that wet snow ice thickness is horizontal ice thickness and can be converted to radial ice thickness.

2.2.3 Test Case Simulation of an Icing Event

To test icing estimates, we simulated a historical storm event that led to icing and power outages in the Northeastern United States, the December 11-12, 2008 event (NEI, 2009). To simulate the test case, we use the European Centre for Medium-Range Weather Forecasts (ECMWF) Re-Analysis, ERA-Interim, (Dee *et al.*, 2011) to drive WRF simulations and initialize the model 12 hours prior to the onset of the event.

Figure 2 shows that observed and simulated ice thicknesses agree in terms of location, while magnitude is slightly larger in the latter. Given observed data reflect horizontal accumulation not radial ice thickness and are from point location

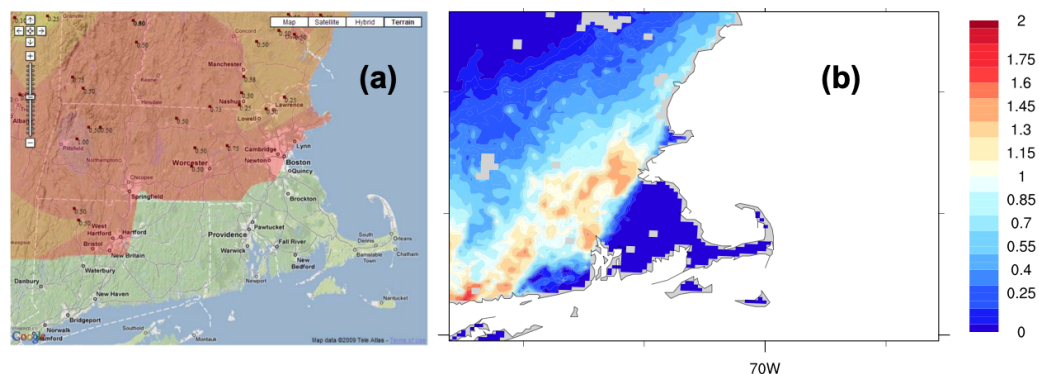


Figure 2. Test Case icing December 11-12 2008: (a) observed ice accumulated thickness as reported NOAA NWS Taunton (NOAA WFO, 2009) (b) modeled accumulated ice thickness.

measurements as opposed to homogeneously gridded data, the good agreement between observations and our simulation justifies the use of our icing estimate in downscaled ESM fields.

3. Climate Projections for 2025-2041 and Changes in Climate

For this project, we simulate a 17-year near future time period between 2025 and 2041. In this section, we summarize the mean and extreme climate (focusing on temperatures, winds and ice accumulation) during the near future time period and provide analysis of climate change compared to the present-day climate (2006-2020), which we obtain from Dr. Komurcu's existing dynamically downscaled CESM historical simulations using the same modeling setup (Komurcu *et al.*, 2018). It is important to note that because the two time periods are close, projected changes are expected to be small. Furthermore, while we use the full time series for both time periods when analyzing mean climate and climate change, when analyzing extremes in the following sections, in order to have meaningful comparisons between the two time periods, we eliminate the first two years of the near future simulations and focus on 2028-2041, which then yields the same length (15 years) time series for both time periods.

3.1 Temperatures

A summary of the mean and extreme characteristics of temperatures for the simulated near future time period between 2025 and 2041 is provided in Figures 3 and 4. **Figure 3** (panel a-c) show the average changes in the daily mean, June-July-August (JJA) mean daily maximum and December-January-February (DJF) mean daily minimum temperatures, respectively.

As expected, we see a temperature gradient exhibiting lower temperatures towards higher latitudes in our simulations (Figure 3). Furthermore, the 3 km-resolution of our simulations allow for the detailed representation of topographical and spatial features which allows us to see the effects of regional and local topography on the spatial distribution of temperatures more clearly (Figures 3 and 4).

We also examine extreme summertime (JJA) daily maximum and wintertime (DJF) daily minimum temperatures (**Figure 4**). Here, we define extreme as the 95th percentile of daily maximum and minimum temperatures. As expected, both maximum and minimum temperatures reveal cooler temperatures towards northern latitudes. Furthermore, cooling effects of high topography (e.g. along the Allegheny Mountains) and coastal areas are evident in both summertime and wintertime extremes (Figure 4).

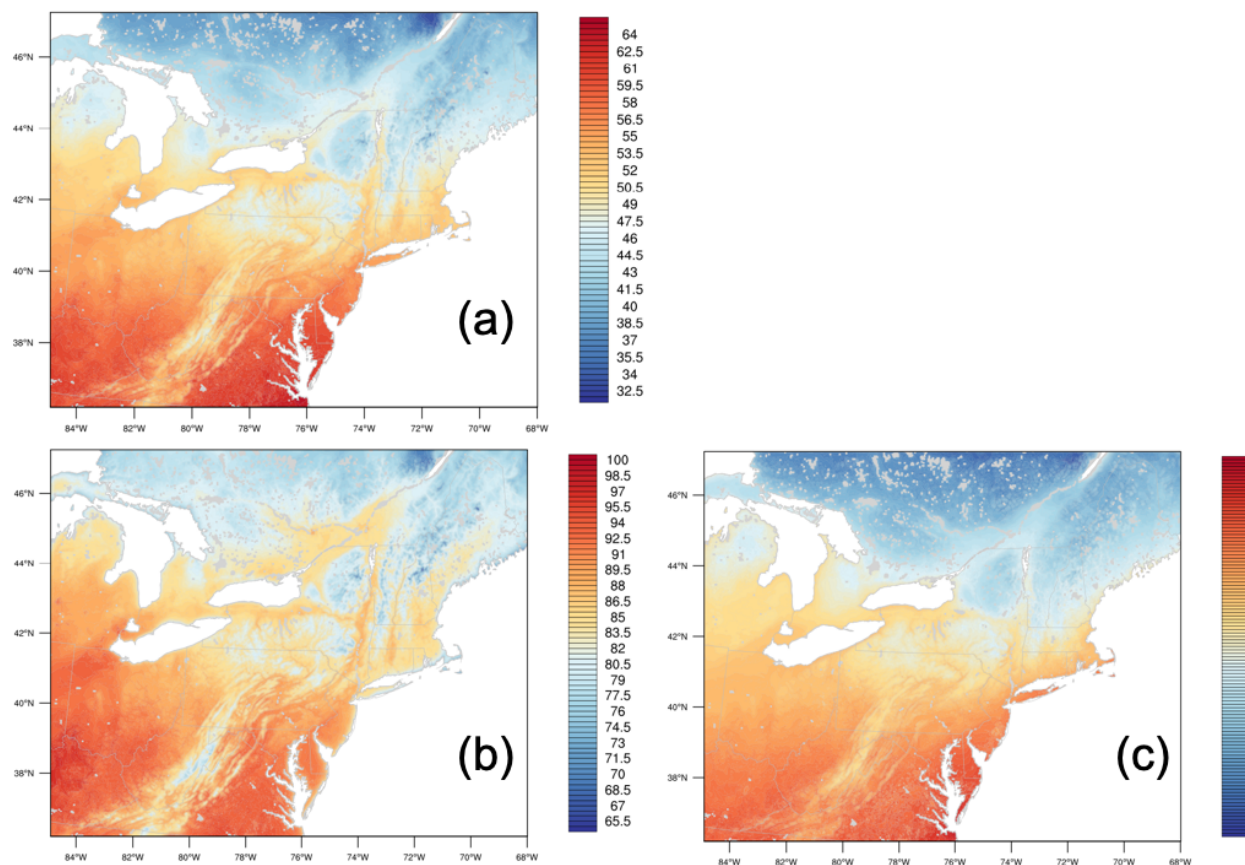


Figure 3. (a) Annual mean Daily mean temperatures (b) June July August (JJA) mean Daily Maximum temperatures and (c) December January February (DJF) mean Daily Minimum temperatures averaged over 2025-2041 [°F].

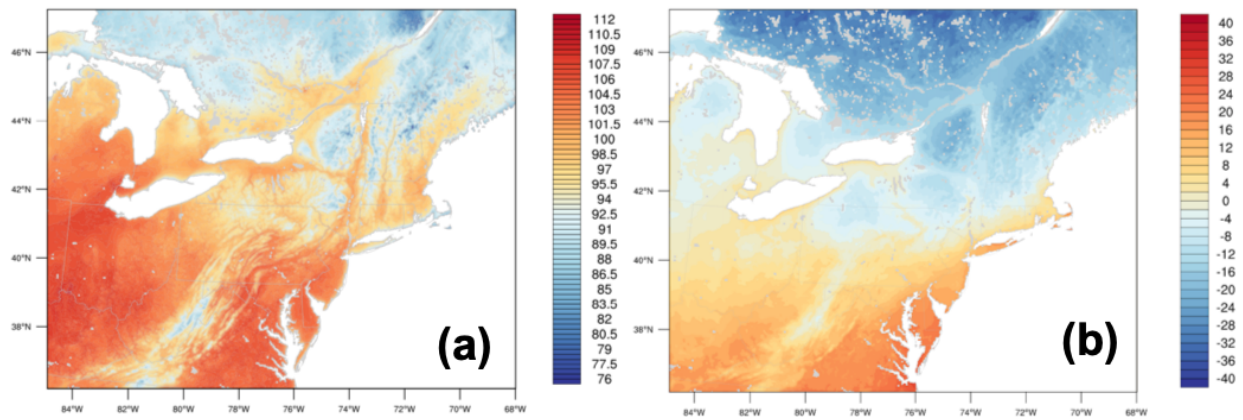


Figure 4. (a) June July August (JJA) daily maximum and (b) December January February (DJF) daily minimum extreme temperatures (95th percentile) between 2025 and 2041 [°F].

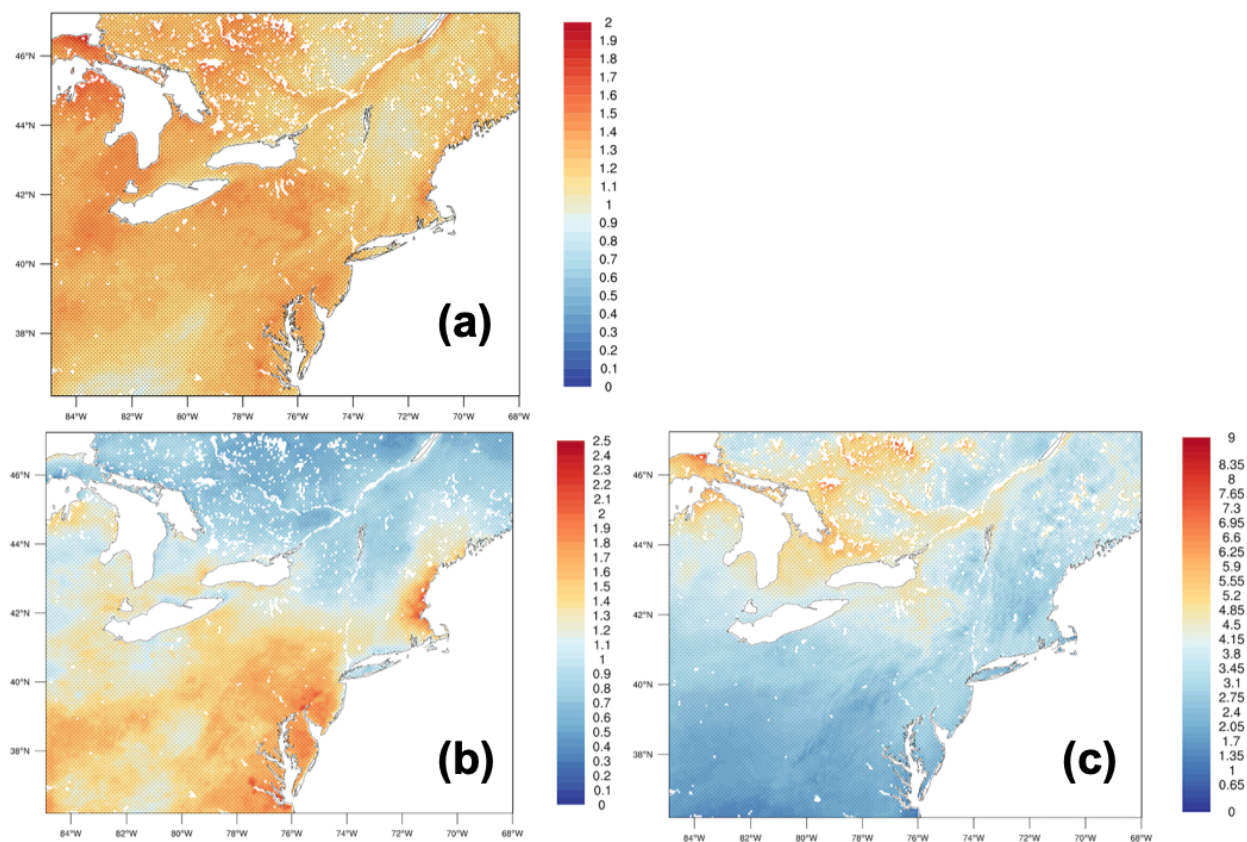


Figure 5. Changes in the (a) annual mean daily mean, (b) June July August (JJA) mean daily maximum and (c) December January February (DJF) mean daily minimum temperatures between 2025-2041 and 2006-2020 [°F]. Stippling reflects statistically significant differences at 95% level using student's t test.

Next, we compare our simulated 17-year, near future time period (2025-2041) to the present-day climate (2006-2020). We find that daily mean temperatures increase over the whole region. The simulated changes are as much as 2°F between the present day and the near future climate (Figure 5a). Summertime maximum temperatures increase as much as 2.5°F and these are primarily intensified towards the South of the region and some along the Northeast

as well as coastal Massachusetts and Maine (Figure 5b). Minimum temperatures also exhibit increases throughout our 3 km resolution domain. The largest changes in wintertime daily minimum temperatures are seen in the interior of the simulation domain along the Great Lakes and interior Canada (Figure 5c).

We also examine the changes in extreme temperatures between the two time periods. We find that summertime

(JJA) extreme daily maximum temperatures increase as much as 4°F between near future and present-day climate and the largest increases are seen within the interior areas of southeastern parts of our domain along the Allegheny Mountains. Similarly, we find that extreme minimum temperatures increase for the entire domain with some of the largest changes in extreme minimum temperatures exhibited around the coasts of Great Lakes (Figure 6b). Hence, in the near future climate, minimum temperatures do not fall as much as they do in present day climate in high-resolution simulations. It is important to note that the analysis here is to showcase what is simulated for the time period. By definition extreme reflects a percentile value here, which is a single value for both time periods, hence a more detailed analysis is desirable for more robust characterization of changes in extremes in the data.

3.2 Conditions for Ice Accumulation on Surfaces

We next examine our estimates of ice accumulation on critical surfaces due to freezing rain and wet snow icing as described in Section 2.2. To visualize potential icing due to

freezing rain and wet snow, we calculate annual maximum ice accumulation for both types of icing and average them through the entire near future time period (Figure 7 a and b).

We find that the magnitude of freezing rain ice accumulation is an order of magnitude smaller in the region for the near future time period in our simulations than wet snow ice accumulation, which is not surprising considering the physical characteristics and occurrence of rain and snow over the region. Furthermore, we find that annual maximum wet snow ice accumulation is predominantly larger over the Northeastern parts of our domain in near future climate, while freezing rain icing exhibits largest values over high topography and around lakes in our simulations for the near future time period (Figure 7).

Comparing near future and present-day climate in our simulations, we find annual maximum magnitude of freezing rain ice accumulation potential to remain the same over most of the domain and increase modestly in to the future with more pronounced increases around Great Lakes, and along the Allegheny Mountains (Figure 8a). Wet snow ice accumulation potential, on the other hand, exhibits both increases and reductions throughout the region and exhibit

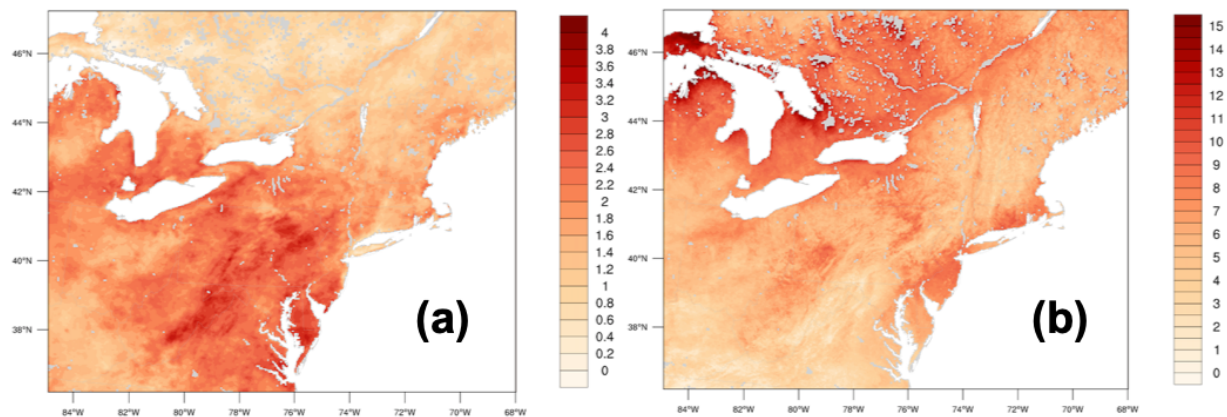


Figure 6. Changes in (a) June July August (JJA) daily maximum, and (b) December January February (DJF) daily minimum extreme temperatures (95th percentile) between 2028-2041 and 2006-2020 [°F].

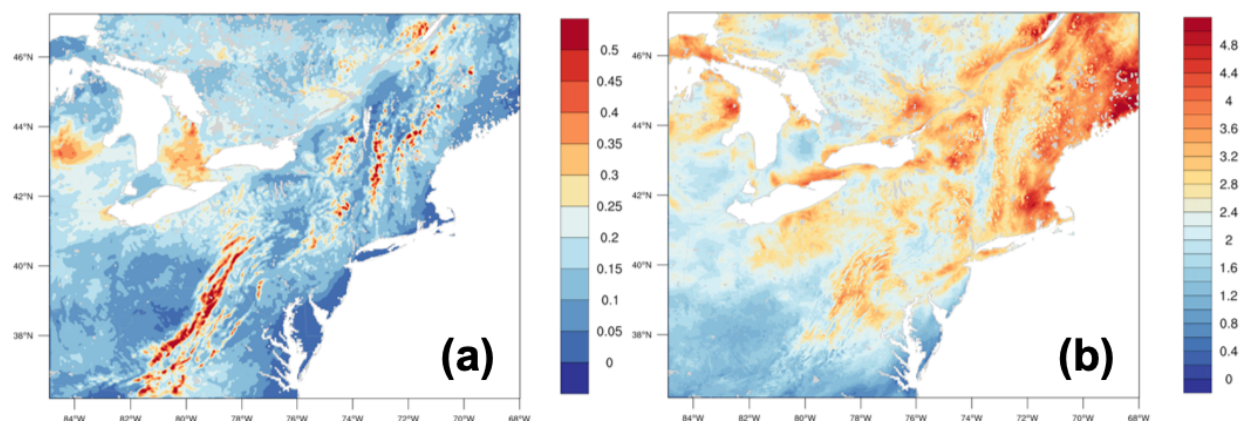


Figure 7. Annual maximum (a) freezing rain radial ice thickness and (b) wet snow horizontal ice thickness [inches] between 2025-2041.

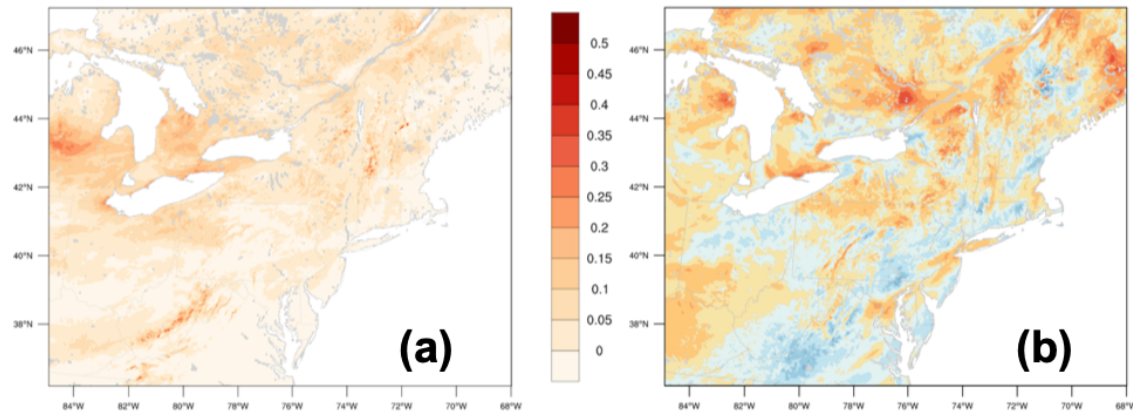


Figure 8. Changes in annual maximum (a) freezing rain radial ice thickness and (b) wet snow horizontal ice thickness [inches] between 2025-2041 and 2006-2020.

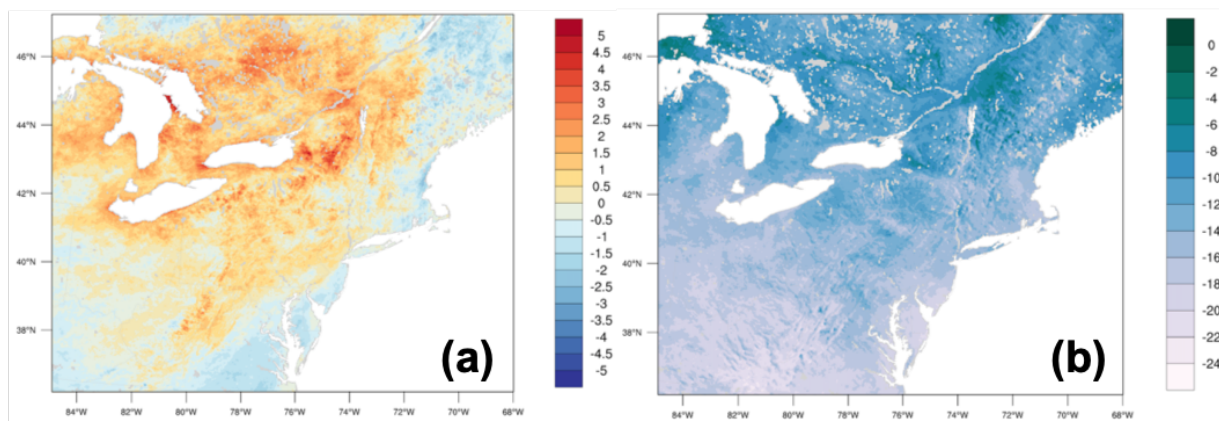


Figure 9. Differences in number of days per year with occurrence of icing due to (a) freezing rain and (b) wet snow between 2025-2041 and 2006-2020.

the largest increases towards the northeastern parts of our domain (**Figure 8b**).

To study the changes in the frequency of conditions suitable for each of the two types of icing, we plotted the changes in the annual number of days per year with occurrence of icing due to (a) freezing rain and (b) wet snow between 2025-2041 and 2006-2020 (**Figure 9**). We find that annual occurrence of conditions conducive to wet snow icing reduces in our simulations over the whole region in the near future climate. Conditions conducive to freezing rain icing occurrence, on the other hand, increase inland, particularly around the Great Lakes, along the Allegheny Mountains and the interior subregions of Pennsylvania, New York and Canada.

3.3 Wind Speeds and Direction

We next investigate surface wind speeds (10 meters). It is important to note that we are using hourly wind data from high-resolution simulations and not wind gusts or maximum winds within the hour. Even though we calculate the latter in our near future climate projections, such information is not available in present day climate

data which prevents us from calculating changes in maximum winds between the two time periods. We present mean surface wind speeds (**Figure 10a**) in 2025-2041 and changes in mean wind speeds compared to present-day climate (2006-2020) (**Figure 10b**). We find that magnitudes of mean wind speeds exhibit small changes in our simulations between near future and the present-day time periods (**Figure 10b**).

We also investigate changes in the direction of the mean wind speed (**Figure 11**) between near future and present-day time periods. We find that the direction of mean winds remains the same throughout the domain between the two time periods (2025-2041 and 2006-2020) in our simulations.

Aside from mean wind speeds, we also examine magnitudes of extreme wind speeds and changes in the magnitude of extreme winds, extreme is defined as the 95th percentiles of daily maximum wind speeds between near future and the present-day time periods (**Figure 12**). We find that the magnitude of extreme wind speeds reach as much as 30 m/s over regions with high topography between 2025 and 2041 (**Figure 12a**) in our projections. Furthermore, we also find

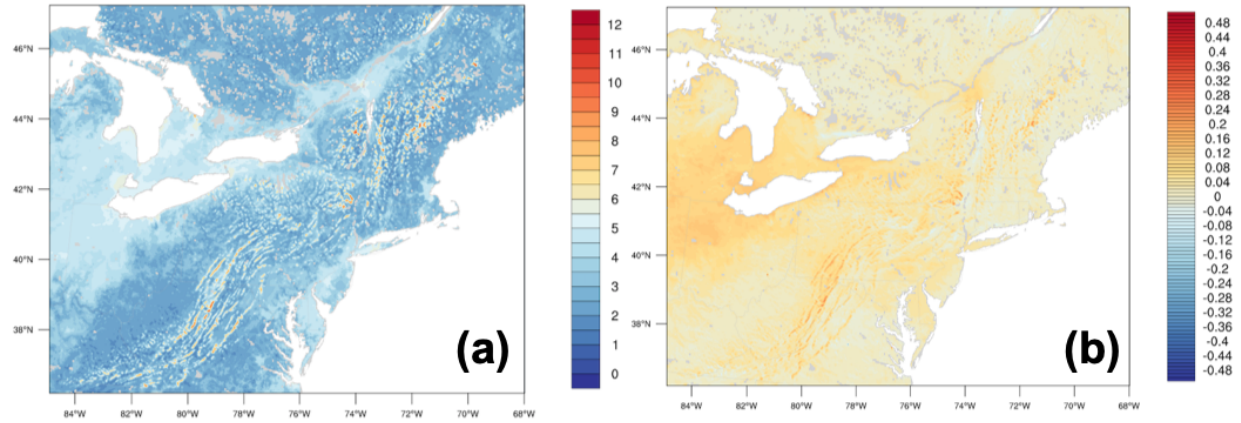


Figure 10. (a) Mean wind speed [m/s] between 2025 and 2041 (b) changes in wind speed between 2025-2041 and (2006-2020).

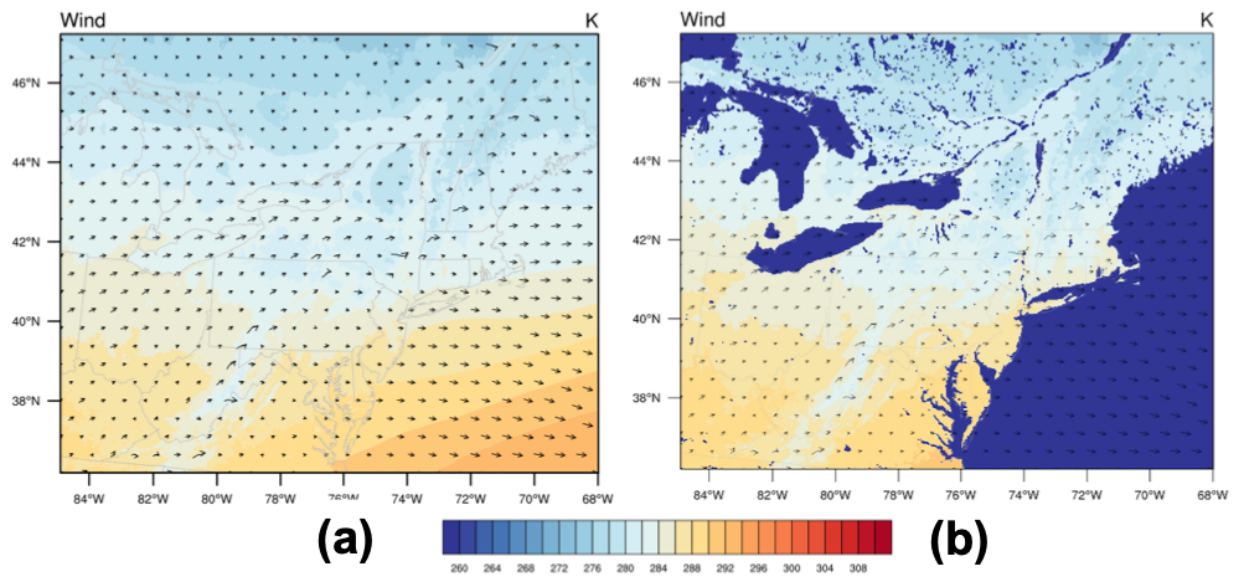


Figure 11. Direction of mean wind speeds (a) 2006-2020 (b) 2025-2041 along with mean surface temperatures (K) (color shaded).

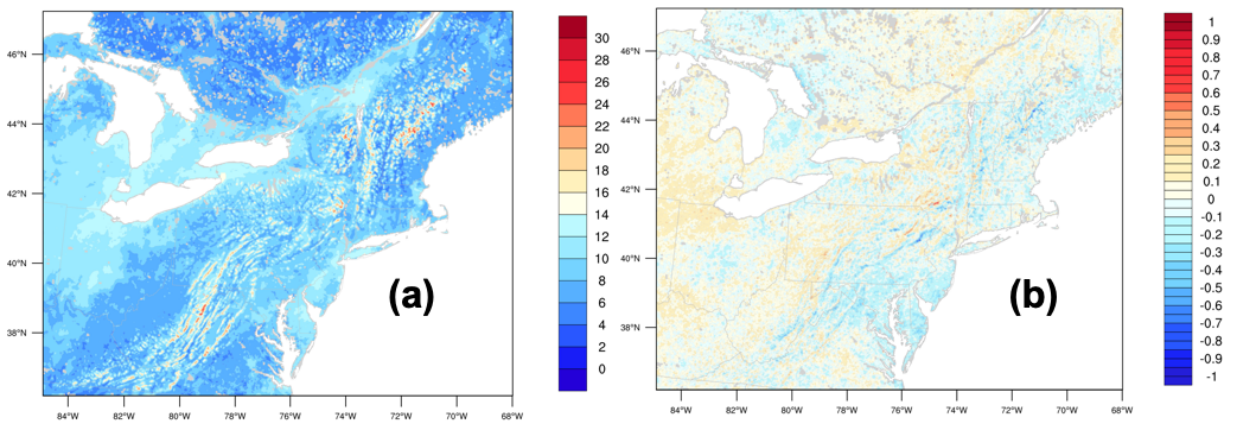


Figure 12. a) Extreme wind speeds [m/s] (95th percentile of winds) between 2028-2041 and b) changes in the extreme wind speeds between 2028-2041 and 2006-2020.

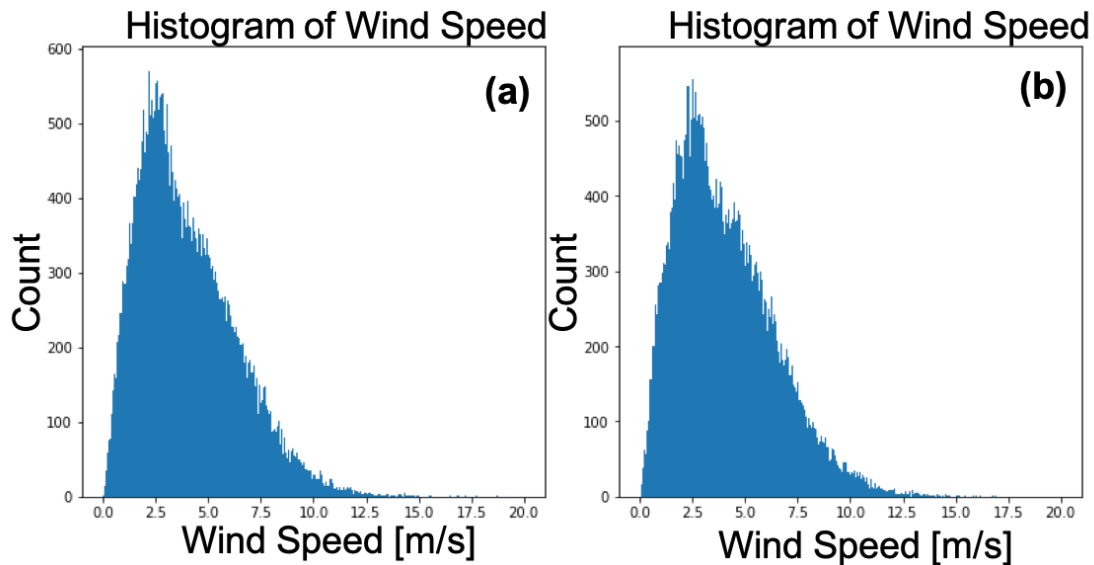


Figure 13. Histogram of wind speeds for (a) present day (2006-2020) and (b) near future (2025-2041) using hourly data for the entire time periods.

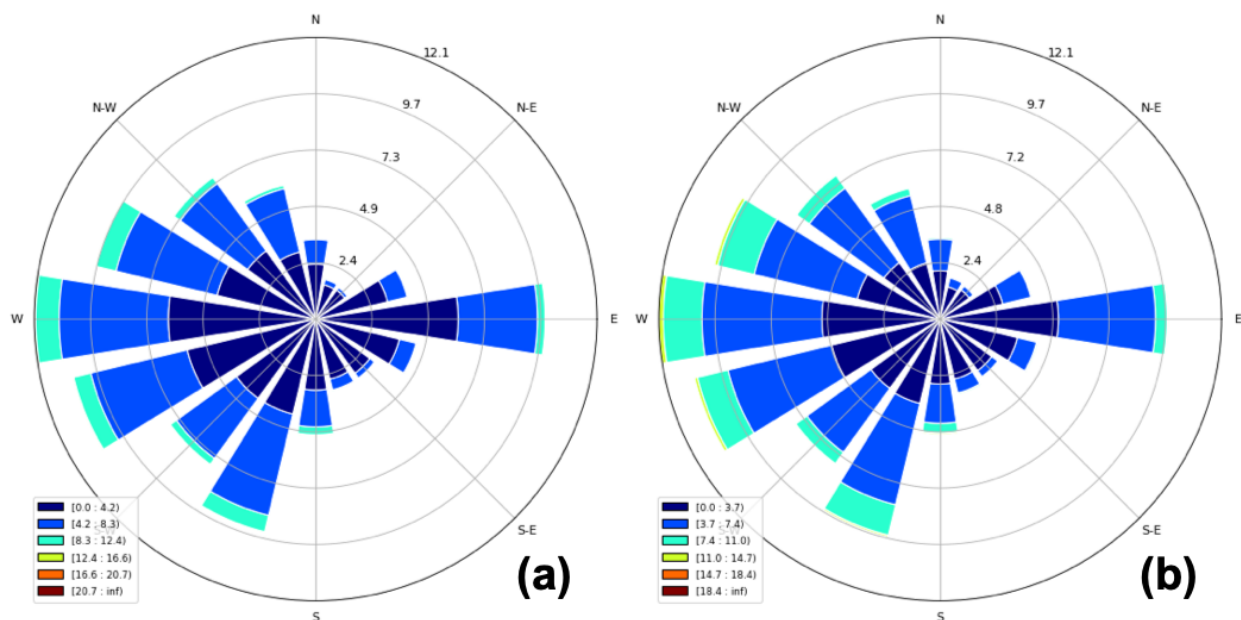


Figure 14. Wind rose (a) Present Day (2006-2020) (b) Near Future (2025-2041) in Syracuse, NY.

that changes in extreme wind speeds between 2028-2041 and 2006-2020 are small in our simulations (Figure 12b).

Next, we focus on a specific location to study potential changes in wind speeds and wind direction between near future and present-day climate in our simulations. We pick Syracuse, NY and focus on a single point representing Syracuse, NY, however, it is also possible to compare wind statistics using a mean of several points surrounding the location.

We present histograms of **hourly** simulated 10-meter wind speeds in Syracuse, NY for present-day climate in **Figure 13a** and near future climate in **Figure 13b**. We find that both

mean and tails of the distribution are quite similar between the two time periods. Hence, we find that magnitude of wind speed and its distribution do not change between the two time periods in our simulations.

To evaluate whether the location experiences any changes in wind direction between 2006-2020 and 2025-2041, we present wind rose for both near future and present-day climate for Syracuse, NY (**Figure 14**). Wind rose is commonly used in meteorology and provides prevalent wind direction along with distributions of wind speeds and direction for a particular location. Plotted wind direction is

meteorological wind direction, in other words, the direction where the wind is coming from. We find that dominant wind direction does not change in Syracuse, NY between 2025-2041 and 2006-2020 in our simulations (Figure 14).

4. Aggregate Average Changes in Temperature, Icing, and Winds

For illustrative purposes, in **Tables 1-3** we report aggregate average changes in temperature, icing and wind over the entire domain. While the impacts on energy infrastructure need to be assessed at particular locations, this aggregate information provides an indication of changes. Relative to the present day (2006-2020) climate, mean temperatures are 1.2°F higher in the 2025-2041 period. All other indicators show increases in temperatures. For icing indicators, we observe an increase in annual freezing rain days (0.3 days for the domain mean) and a decrease in annual wet snow days (13.2 days for the domain mean). For wind indicators, changes in mean wind speeds and extreme wind speeds are relatively small. The hourly high-resolution climate projections data we created in this study allow us to calculate these indicators for particular locations to assess potential impacts on infrastructure in those locations.

5. Potential Impacts of Projected Changes on Electric Grid Infrastructure and Design Thresholds

To analyze climate risks on infrastructure, specific information on climatic thresholds for safe operation of electric grid infrastructure and comprising equipment is needed. Basic provisions for safeguarding from hazards arising from the installation, operation, or maintenance of conductors and equipment in electric supply stations, and overhead and underground electric supply and communication lines are available in the National Electric Safety Code (NESC) (IEEE, 2017) and system operator standards (see, for example, ISO (2020) for the New England ISO transmission planning guide). While the goal of this report is to provide future climate data to assess the necessary changes for infrastructure planning, for illustrative purposes we also performed several calculations for the entire domain against the thresholds set by NESC and ISO. We stress the illustrative nature of our calculations because the design of electric infrastructure and equipment is based on certain climatic assumptions for different zones within the United States. A comprehensive analysis should be performed based on the exact location of the assets and in collaboration with asset maintainers/managers.

Table 1. Aggregate mean changes over the entire domain for select temperature indicators from the Present Day (2006-2020) to the Near Future (2025-2041) projections. JJA – June, July, August. DJF – December, January, February.

Temperatures	Changes in Mean T [°F]	Changes in JJA Maximum T [°F]	Changes in DJF Minimum T [°F]
Domain Mean	1.2	1.1	3.4
Domain Max	1.9	2.2	8.4
Domain Min	0.7	0.3	0.5

Table 2. Aggregate mean changes over the entire domain for select icing indicators from the Present Day (2006-2020) to the Near Future (2025-2041) projections.

Icing	Changes in Annual Maximum Freezing Rain Icing [inches]	Changes in Annual Maximum Wet Snow Icing [inches]	Changes in Annual Freezing Rain Days	Changes in Annual Wet Snow Days
Domain Mean	0	0.2	0.3	-13.2
Domain Max	0.5	2.7	5.9	-1.6
Domain Min	-0.5	-2.5	-3.5	-23.8

Table 3. Aggregate mean changes over the entire domain for select wind indicators from the Present Day (2006-2020) to the Near Future (2025-2041) projections.

Winds	Changes in Mean Wind Speed [m/s]	Changes in Extreme Wind Speed [m/s]
Domain Mean	0.03	0
Domain Max	0.4	-1.2
Domain Min	-0.5	-1.1

We first explore an annual exceedance of temperature thresholds during the summers of the near future (2025-2041) time period. **Figure 15** shows an annual number of days temperatures exceed 82°F, 90.4°F and 94.2°F, respectively. These thresholds are chosen for the following reasons. The threshold of 82°F is one of the parameters used in the planning of the overhead lines and it is the temperature for which the maximum sag for overhead lines is calculated (IEEE, 2017). The latter two thresholds are based on a transmission technical guide (ISO, 2020). The guide highlights that a peak load with a 50/50 peak load, meaning that a 50% chance of being exceeded because of weather conditions, is expected to occur in New England at a temperature of 90.4°F. The corresponding number for a (90/10) peak load (with 10% chance of being exceeded) is 94.2°F.

We also calculate an annual number of days where winter minimum temperatures reach subfreezing temperatures ($<32^{\circ}\text{F}$ or $<0^{\circ}\text{C}$) (**Figure 16a**) and magnitudes below 0°F (**Figure 16b**). Both thresholds are used in design codes to incorporate regional ice accumulation limits in the design and are evaluated with 0.25, 0.5 inches or 1 inches of ice accumulation for the Northeastern United States (IEEE, 2017). Hence, we also present annual exceedances for 0.25 inches for our estimates of both freezing rain and wet snow ice accumulation (**Figure 17**). Finally, we provide annual exceedance of wind thresholds for wind speeds of 30 and 40 mph (**Figures 18a and 18b**).

We intentionally omit interpretations of stand-alone and combined effects of winds, temperatures and ice accumulation on infrastructure. To make valid assessments of specific climate risks on infrastructure, experts at utility companies responsible for the specific infrastructure need to be involved in the analysis. Here we provide the analysis of our high-resolution data using exceedance thresholds specified in particular safety codes. Hence, our data at 3km by 3km resolution can be used for analysis of impacts on specific assets and the environmental conditions in their vicinity for infrastructure planning purposes (see Appendix A for a list of variables).

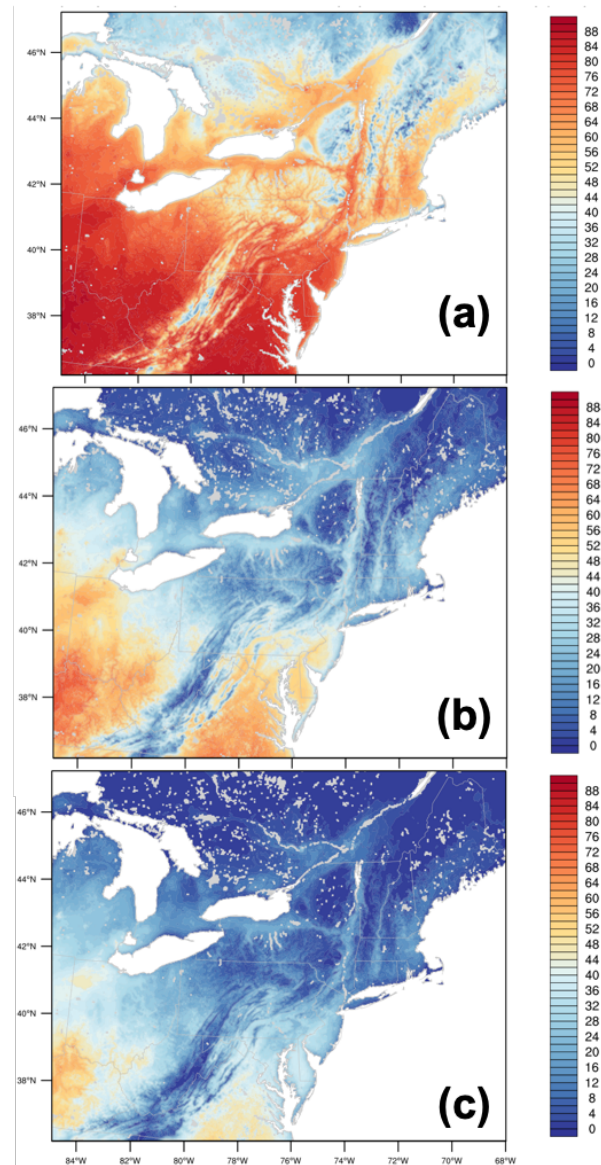


Figure 15. Annual number of summer days (JJA) daily maximum temperatures exceed: (a) 82°F (27.78°C), (b) 90.4 °F (32.4°C), (c) 94.2 °F (34.56°C) between 2025-2041.

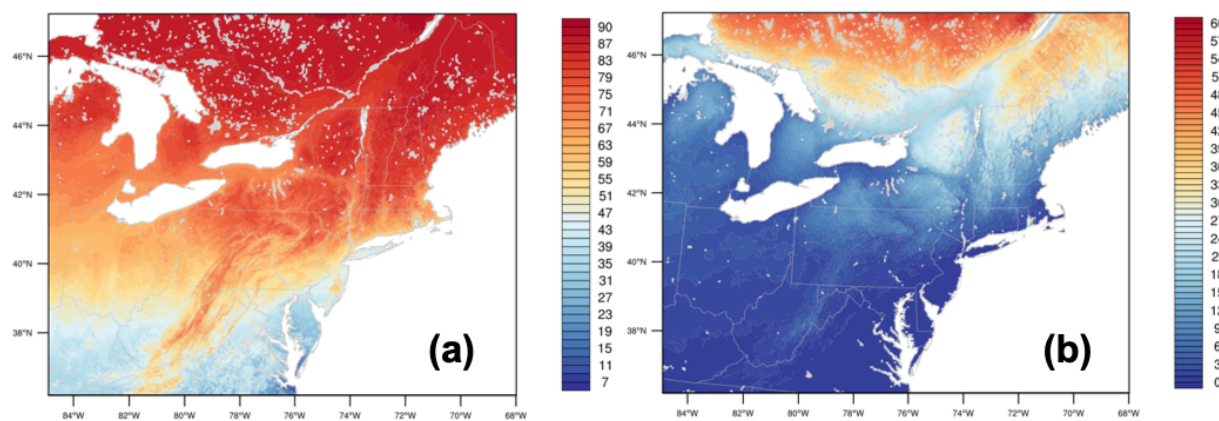


Figure 16. Annual number of winter (DJF) days daily minimum temperatures are: (a) sub 0°C and (b) sub 0°F between 2025-2041.

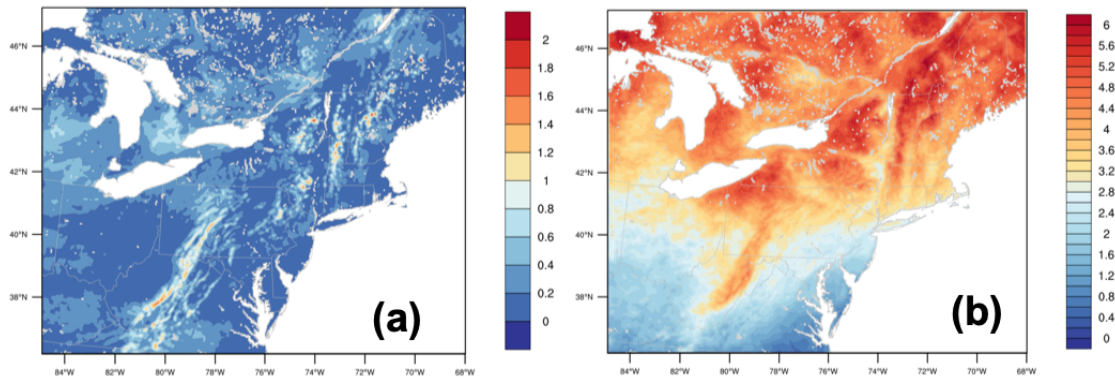


Figure 17. Number of months per year where: (a) freezing rain icing radial ice thickness, (b) wet snow horizontal ice thickness exceed 0.25 inches between 2025-2041.

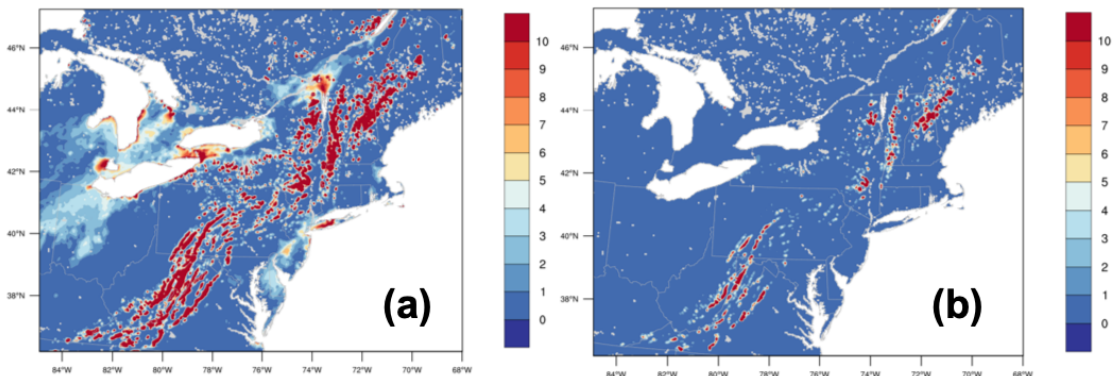


Figure 18. Annual number of hours wind speeds exceed: (a) 30 mph and (b) 40 mph between 2025-2041.

6. Concluding Remarks and Suggestions for Future Analysis

Our report presents mean and extreme characteristics of the near future (2025-2041) climate in the Northeastern United States obtained through dynamical downscaling of the projections of CESM under a high impact scenario. The data generated for this work is at hourly temporal resolution and the size of the model output data is about 100 Terabytes. The available data at 3km by 3km geographic resolution include among many other variables the projections of temperature, wind speeds, wind direction, snow depth, snowfall, precipitation at surface, atmospheric pressure, water vapor, and relative humidity. We also performed determination of icing conditions (ice accumulation on surfaces) using historical and future climate projections (1 Terabyte).

In this report we presented an analysis of changes in climate variables that could affect energy infrastructure such as winds, temperatures and ice accumulation. While the climate change analysis provided here is an assessment of overall changes in downscaled projections within the highest resolution domain (Figure 1), it is possible to make more detailed assessments for specific locations using the high spatial resolution, hourly data products we created. We recommend asset engineers and managers to collaborate with atmospheric and climate scientists to incorporate such detailed climate information in asset management.

During our project, we also discovered a lack of available historical icing data. For better assessments of infrastructure resiliency, a dense network of historical measurements is necessary. Therefore, it would be extremely helpful to install cameras and sensors on electric grid infrastructures to routinely measure and report depths of ice accumulation, height of surface where ice accumulation occurs (or height of measurement device), as well as accompanying weather elements such as temperatures, winds and relative humidity. Furthermore, while it is possible to incorporate direct ice growth in numerical weather prediction models (which is also the basis of our climate modeling), such simulations are computationally expensive in our high-resolution climate modeling context due to large number of years simulated in high resolution and the need to include even more detailed microphysics as well as increased number of vertical atmospheric levels in modeling. Success of such modeling efforts also heavily rely on the availability of the above-mentioned data. Simulating climate change at high resolution (with convection permitting scales like the ones we present here) comes at a heavy computational expense. Our dynamically downscaled projections of CESM are state-of-the-art. The projections are unique in their solid foundations to enable infrastructure planners to make assessments of climate change at local scales and understanding future climate conditions is imperative for electric grid utilities. While

our simulations are most certainly useful in studying local climate change in detail, including projections from more than one ESM for at least 30 years and under different future emissions scenarios would help to frame the uncertainty and provide a more comprehensive picture of the potential future changes, which would then allow more robust assessments of climate risks in collaboration with asset managers/engineers. We call for an increased support of such high-resolution climate studies and collaborations across disciplines to provide decision making management with robust information about safety of future operations that thoroughly consider physical risks of climate change on infrastructure.

7. References

- Blunden, J. and D. S. Arndt, Eds., 2019, State of the Climate in 2018. *Bull. Amer. Meteor. Soc.*, 100 (9), Si–S305, doi:10.1175/2019BAMSStateoftheClimate.1.
- Bruyère, C.L., J.M. Done, G.J. Holland & S. Fredrick (2014). Bias corrections of global models for regional climate simulations of high-impact weather. *Climate Dynamics*, 43(7-8): 1847–1856 (doi: 10.1007/s00382-013-2011-6).
- Dee, D.P., S.M. Uppala, A.J. Simmons, P. Berrisford, P. Poli, S. Kobayashi *et al.* (2011). The ERA-Interim reanalysis: Configuration and performance of the data assimilation system. *Quarterly Journal of the Royal Meteorological Society*, 137(656): 553–597.
- Farzaneh, M. (2008). *Atmospheric Icing of Power Networks*. Springer, ISBN: 978-1-4020-8530-7.
- Flato, G., J. Marotzke, B. Abiodun, P. Braconnot, S.C. Chou, W. Collins, P. Cox, F. Driouech, S. Emori, V. Eyring, C. Forest, P. Gleckler, E. Guilyardi, C. Jakob, V. Kattsov, C. Reason & M. Rummukainen (2013). Evaluation of climate models. In T. F. Stocker, *et al.* (Eds.), *Climate change 2013: The physical science basis. Contribution of Working Group I to the Fifth Assessment Report of the Intergovernmental Panel on Climate Change* (Vol. 9, pp. 741–866). Cambridge, UK and New York: Cambridge University press.
- Giorgi, F. (1990). Simulation of regional climate using a limited area model nested in a general-circulation model. *J. Clim.*, 3(9): 941–963.
- IEEE (2017). 2017 National Electric Safety Code (NESC). Institute of Electrical and Electronics Engineers.
- IPCC (2013). Summary for Policymakers. In: *Climate Change 2013: The Physical Science Basis*. Contribution of Working Group I to the Fifth Assessment Report of the Intergovernmental Panel on Climate Change [Stocker, T.F., D. Qin, G.-K. Plattner, M. Tignor, S.K. Allen, J. Boschung, A. Nauels, Y. Xia, V. Bex and P.M. Midgley (eds.)]. Cambridge University Press, Cambridge, United Kingdom and New York, NY, USA.
- ISO (2020). ISO New England Inc. Transmission Planning Technical Guide, Revision 6.1. <https://www.iso-ne.com/system-planning/transmission-planning/transmission-planning-guides>
- Jones, K.F. (1998). A simple model for freezing rain ice loads. *Atmos. Res.*, 46, 87–97.
- Komurcu, M., K. Emanuel, M. Huber and R. Acosta (2018). High-resolution climate projections for the northeastern United States using dynamical downscaling at convection-permitting scales. *Earth Space Sci.*, 5, 801–826 (doi: 10.1029/2018EA000426).
- Komurcu, M., C.A. Schlosser, I. Alshehri, T. Alshahrani, W. Alhayaza, A. Alsaati and K. Strzepak (2020). Mid-Century Changes in the Mean and Extreme Climate in the Kingdom of Saudi Arabia and Implications for Water Harvesting and Climate Adaptation. *Atmosphere*, 11, 1068 (doi: 10.3390/atmos11101068).
- Koren, V., J. Schaake, K. Mitchell, Q.-Y. Duan, F. Chen and J. Baker (1999). A parameterization of snowpack and frozen ground intended for NCEP weather and climate models. *J. Geophys. Res.*, 104(D16): 19569–19585 (doi:10.1029/1999JD900232).
- Monaghan, A.J., D.F. Steinhoff, C.L. Bruyère & D. Yates (2014). NCAR CESM global Bias-corrected CMIP5 output to support WRF/MPAS research. Research Data Archive at the National Center for Atmospheric Research, Computational and Information Systems Laboratory (doi: 10.5065/D6DJ5CN4).
- Musilek, P., D. Arnold and E.P. Lozowski (2009). An ice accretion forecasting system (IAFS) for power transmission lines using numerical weather prediction. *Sci. Online Lett. Atmos.*, 5, 25–28.
- NEI (2009). New Hampshire December 2008 Ice Storm Assessment Report. October 28, 2009, NEI Electric Power Engineering.
- NOAA NWS, Taunton, WFO Storm Series Report: 2009-01. Analysis of the December 11-12, 2008 Destructive Ice Storm across Interior Southern New England.
- Pruppacher, H.R. and J.D. Klett (2010). *Microphysics of Clouds and Precipitation*. Springer, ISBN 978-0-306-48100-0.
- Sanders, K.J. & B.L. Barjenbruch (2016). Analysis of Ice-to-Liquid Ratios during Freezing Rain and the Development of an Ice Accumulation Model. *Weather and Forecasting*, 31(4): 1041-1060.
- Skamarock, W.C., J.B. Klemp, J. Dudhia, D.O. Gill, D.M. Barker, M. Duda *et al.* (2008). A Description of the Advanced Research WRF Version 3 (technical note NCAR/TN-475+STR). Boulder CO: National Center for Atmospheric Research (doi: 10.5065/D68S4MVH).
- Sundin, E. & L. Makkonen (1998). Ice Loads on a Lattice Tower Estimated by Weather Station Data. *Journal of Applied Meteorology*, 37(5): 523-529.
- Wilby, R.L., T.M.L. Wigley, D. Conway, P.D. Jones, B.C. Hewitson, J. Main and D.S. Wilks (1998). Statistical downscaling of general circulation model output: A comparison of methods. *Water Resour. Res.*, 34(11): 2995–3008 (doi:10.1029/98WR02577).

Appendix A.

In Appendix A, we provide a list of select variables created for our analysis of climate change impacts on energy infrastructure in this project for the time period between 2025 and 2041. The modeling has been performed at the MIT's Svante high performance computing system. Full model output data contains numerous additional 2-dimensional (latitude-longitude) and 3-dimensional (latitude, longitude, height) climate variables than those listed here and are saved

hourly for 17 years with a file size of about 100 Terabytes. The icing calculations for wet snow and freezing rain icing take additional 500Gb. The data for the future time period (2025-2041) remain at MIT and can be shared upon agreement. The data for the present day climate (2006-2020) remains at MIT and can be requested from the University of New Hampshire Data Distribution Center (UNH DDC).

Variable Number	
1	Ground Level Temperature (2-D) [K]
	Temperature variation at various elevations per unit of time:
2	Temperature (3-D) [K]
3	Temperature at 2 meters [K]
4	Temperature max at 2 meters [K]
5	Temperature min at 2 meters [K]
	Average Wind Speed [m/s]:
6	Wind speed (3-D)
7	10 meter wind speed (2-D)
	Maximum Snow Volume per Day:
8	Snow Water Equivalent (2-D) [kg/m ²]
9	Snow depth [mm]
10	Snowfall [mm]
	Average Snowfall per Year:
11	Snowfall [mm]
12	Graupel [mm]
	Precipitation at Surface (2-D) [mm]:
13	Snowfall [mm]
14	Rain [mm]
15	Graupel [mm]
	Atmospheric Pressure:
16	Pressure (3-D)
17	Surface Pressure (2-D) [Pa]
	Water vapor Mixing Ratio:
18	Water vapor mixing ratio at 2 meters [kg/kg]
	Maximum Wind Speed [m/s]:
19	Level Ground
20	Level 10m
21	Level 15m (50 ft)
22	Level 45m (150 ft)
23	Wind Direction of Maximum Winds at levels listed in lines 19-22
24	Relative Humidity
	Determination of Icing Conditions in Climate Simulations
25	To determine icing conditions for wet snow and freezing rain icing, we will use our model simulated (WRF) rain and snow precipitation rates [mm water equivalent] in combination with temperatures and winds. Then, we will use this information to estimate the accumulation of ice [mm] on surfaces.

Joint Program Report Series - Recent Articles

For limited quantities, Joint Program Reports are available free of charge. Contact the Joint Program Office to order.

Complete list: <http://globalchange.mit.edu/publications>

- 352. Toward Resilient Energy Infrastructure: Understanding the Effects of Changes in the Climate Mean and Extreme Events in the Northeastern United States.** *Komurcu & Paltsev, Jun 2021*
- 351. Meeting Potential New U.S. Climate Goals.** *Yuan et al., Apr 2021*
- 350. Hydroclimatic Analysis of Climate Change Risks to Global Corporate Assets in Support of Deep-Dive Valuation.** *Strzepek et al., Apr 2021*
- 349. A Consistent Framework for Uncertainty in Coupled Human-Earth System Models.** *Morris et al., Mar 2021*
- 348. Changing the Global Energy System: Temperature Implications of the Different Storylines in the 2021 Shell Energy Transformation Scenarios.** *Paltsev et al., Feb 2021*
- 347. Representing Socio-Economic Uncertainty in Human System Models.** *Morris et al., Feb 2021*
- 346. Renewable energy transition in the Turkish power sector: A techno-economic analysis with a high-resolution power expansion model, TR-Power.** *Kat, Feb 2021*
- 345. The economics of bioenergy with carbon capture and storage (BECCS) deployment in a 1.5°C or 2°C world.** *Fajardy et al., Nov 2020*
- 344. Future energy: In search of a scenario reflecting current and future pressures and trends.** *Morris et al., Nov 2020*
- 343. Challenges in Simulating Economic Effects of Climate Change on Global Agricultural Markets.** *Reilly et al., Aug 2020*
- 342. The Changing Nature of Hydroclimatic Risks across South Africa.** *Schlosser et al., Aug 2020*
- 341. Emulation of Community Land Model Version 5 (CLM5) to Quantify Sensitivity of Soil Moisture to Uncertain Parameters.** *Gao et al., Feb 2020*
- 340. Can a growing world be fed when the climate is changing?** *Dietz and Lanz, Feb 2020*
- 339. MIT Scenarios for Assessing Climate-Related Financial Risk.** *Landry et al., Dec 2019*
- 338. Deep Decarbonization of the U.S. Electricity Sector: Is There a Role for Nuclear Power?** *Tapia-Ahumada et al., Sep 2019*
- 337. Health Co-Benefits of Sub-National Renewable Energy Policy in the U.S.** *Dimanchev et al., Jun 2019*
- 336. Did the shale gas boom reduce US CO₂ emissions?** *Chen et al., Apr 2019*
- 335. Designing Successful Greenhouse Gas Emission Reduction Policies: A Primer for Policymakers – The Perfect or the Good?** *Phillips & Reilly, Feb 2019*
- 334. Implications of Updating the Input-output Database of a Computable General Equilibrium Model on Emissions Mitigation Policy Analyses.** *Hong et al., Feb 2019*
- 333. Statistical Emulators of Irrigated Crop Yields and Irrigation Water Requirements.** *Blanc, Aug 2018*
- 332. Turkish Energy Sector Development and the Paris Agreement Goals: A CGE Model Assessment.** *Kat et al., Jul 2018*
- 331. The economic and emissions benefits of engineered wood products in a low-carbon future.** *Winchester & Reilly, Jun 2018*
- 330. Meeting the Goals of the Paris Agreement: Temperature Implications of the Shell Sky Scenario.** *Paltsev et al., Mar 2018*
- 329. Next Steps in Tax Reform.** *Jacoby et al., Mar 2018*
- 328. The Economic, Energy, and Emissions Impacts of Climate Policy in South Korea.** *Winchester & Reilly, Mar 2018*
- 327. Evaluating India's climate targets: the implications of economy-wide and sector specific policies.** *Singh et al., Mar 2018*
- 326. MIT Climate Resilience Planning: Flood Vulnerability Study.** *Strzepek et al., Mar 2018*
- 325. Description and Evaluation of the MIT Earth System Model (MESM).** *Sokolov et al., Feb 2018*
- 324. Finding Itself in the Post-Paris World: Russia in the New Global Energy Landscape.** *Makarov et al., Dec 2017*
- 323. The Economic Projection and Policy Analysis Model for Taiwan: A Global Computable General Equilibrium Analysis.** *Chai et al., Nov 2017*
- 322. Mid-Western U.S. Heavy Summer-Precipitation in Regional and Global Climate Models: The Impact on Model Skill and Consensus Through an Analogue Lens.** *Gao & Schlosser, Oct 2017*
- 321. New data for representing irrigated agriculture in economy-wide models.** *Ledvina et al., Oct 2017*
- 320. Probabilistic projections of the future climate for the world and the continental USA.** *Sokolov et al., Sep 2017*
- 319. Estimating the potential of U.S. urban infrastructure albedo enhancement as climate mitigation in the face of climate variability.** *Xu et al., Sep 2017*